Supporting information for manuscript

Cervical Cancer Long-term G_1 Cell Cycle Arrest Induced by Co-Immobilized TNF-α Plus IFN-γ Polymeric Drugs

Wuya Chen,[1Δ] Wenwen Wang,[2Δ] Liyi Chen,[1] Jiamei Chen,[1] Xinhua Lu,[1] Zhibin Li,[3] Baoyan Wu,[4,5] Liang Yin,[1] and Yan-Qing Guan[1,4,5**]

Affiliations of authors: 1. School of Life Science, South China Normal University, Guangzhou 510631 (P. R. China), 2. Guangdong Industry Technical College, Guangzhou 510300 (P. R. China), 3. Center for Biomedical Materials and Interfaces, Shenzhen Institutes of Advanced Technology, Chinese Academy of Sciences, Shenzhen 518055 (P. R. China) 4. MOE Key Laboratory of Laser Life Science & Institute of Laser Life Science, College of Biophotonics South China Normal University, Guangzhou 510631 (P. R. China), 5. Joint Laboratory of Laser Oncology with Cancer Center of Sun Yet-sen University, South China Normal University, Guangzhou 510631 (P. R. China),

Δ These three authors contributed equally to this work.

Correspondence to: Yan-Qing Guan, PhD, School of Life Science, South China Normal University, Guangzhou 510631, P. R. China, (E-mail: guanyq@scnu.edu.cn)

Additional Experimental Section

Dead cells analysis

The cells were grown in RPMI 1640 medium (Gibco BRL) with 10% fetal calf serum, supplemented with 0.03 μg/ml penicillin and 0.05 μg/ml streptomycin. Fluorescein diacetate (FDA) was dissolved in acetone solution up to a concentration of 5 mg/ml in 4 ^{o}C, and the final concentration was 1mg/ml. Also, propidium iodide (PI) was dissolved in PBS solution up to a concentration of 1mg/ml in 4 ^{o}C, and the final concentration was 10 μg/ml. Then 0.1 ml FDA and 0.1 ml PI were placed in cell samples for 10 min. After that, the cell samples were cleaned five minutes for three times. Then cells were observed with fluorescence microscope. Living cells are in green and dead cells are in red.

Cell cycle analysis

First, the cells were seeded at 1×10^5 cells/ml into 24-well polystyrene culture plate with serum-free medium and induced by adding the nature TNF-α plus IFN-γ, and co-immobilized them on PSt or NPs to a final concentration of 200 ng/well and 20 ng/well. After stimulated by the TNF-α plus IFN-γ for 24 h, 72 h and 144 h, respectively, these cells were washed three times using phosphate-buffer saline (PBS), and then harvested and fixed in ice-cold 70% ethanol for 12 h. Subsequently, the cells were then stained with primary and secondary antibodies, and one- or two-dimensional flow cytometry (FCM) was performed. they were re-suspended in PBS containing propidium iodide and RNase A, and analyzed by FCM. Data were analyzed using Cell Quest, FlowJo and Modfit software.

Western blotting analysis

HeLa, SiHa or CaSki cells were lysed in extraction buffer (10 mM Tris (pH7.4), 150 mM NaCl, 1%Triton x-100, 5 mM EDTA (pH8.0)). Protein samples were separated by SDS-PAGE (12%) and electro-transferred onto NC (nitrocellulose) membrane (Beijing Zhongshan Golden Biotechnology Co., China). The expression of proteins was analyzed using antibodies to p21, p-p21, p27, p-p27, p53, Bax, Bcl-2, p57, GADD45A, RBL2, RB1, CDK2, CDK4, CDK6, cyclinD, cyclinE, E2F-1, and pRB (Beijing Zhongshan Golden Biotechnology Co.,

China). The blots were incubated with appropriate secondary antibodies conjugated to alkaline phosphatase (ALP) peroxidase (Wuhan Boster Biological Technology Co., China) and developed using ALP reagent (Beyotime Institute of Biotechnology, China). The protein levels were normalized by re-probing the blots with antibody to β-actin (Wuhan Boster Biological Technology Co., China).

Immunohistochemistry analysis

HeLa cells or tumor samples were collected into an Eppendorf tube of 1.5 ml and put in 10% neutral buffered formalin for 12 h. Then they were stained with eosin for 1 min. Three micrometer-thick sections were cut onto positive-charged slides and used for immunohistochemical detection of p27, p21 or Ki67. Briefly, after the deparaffinization in xylene and rehydration through graded alcohols, these sections were microwaved in 0.01 M citrate buffer (pH 6.0) for 15 min. Endogenous peroxidase activity was blocked by immersion in 0.03% H_2O_2 with methyl alcohol for 15 min, where 10% normal rabbit (for mouse primary antibodies) or goat serum (for rabbit primary antibodies) was utilized to avoid non-specific reaction. These sections were then incubated using the primary antibodies for 2-3 h. After washing with PBS, biotinylated anti-muse or rabbit IgG was applied for 20 min at room temperature. The peroxidase-conjugated- streptavidin solution was subsequently applied for 30 min and visualized using 0.05% 3'-3' diaminobenziine (DAB). The counterstaining was performed using hematoxylin. The breast cancer cell known to be positive for p27 or p21 over-expression was used as a positive control. For a negative control, the primary antibody was replaced by a nonspecific negative control antibody.

Immunofluorescence analysis

Cells were washed twice with PBS, fixed with 10% paraformaldehyde for 20 min at room temperature, and permeabilized using 1% Triton-X 100 for 15 min and blocked with PBS containing 1% BSA and 10% cattleserum for 30 mins. Subsequently, they were incubated with appropriately diluted antibodies to p27, p21 (Beijing Zhongshan Golden Biotechnology Co; China) overnight, washed and incubated with corresponding secondary antibodies labeled with cyanine 3 (CY3) for 1 h. Finally, they were washed with PBS, stained

with 4,6-diamidino-2-phenylindole (DAPI) (0.5 μg/ml) and viewed under fluorescence microscopy. The controls are comprised of cells processed without primary antibody.

Real-time fluorescent quantitative PCR analysis

The relative level of p27, p21, or p57 mRNA in HeLa, SiHa or CaSki cells was examined by quantitative RT-PCR (SYBR Green) (ABI 3900, High-Throughput DNA/RNA Synthesizer; ABI 9700, PCR instrument; ABI 7500, fluorescent quantitative PCR instrument; Applied Biosystems, USA). The cells were treated by co-immobilized or free TNF-α plus IFN-γ for 24, 72, or 144 hours.

First, the following primers of p27, p21, or p57 designed with Primer Express 2.0 Software were used for the PCR step: (1) p27, p21, p57 sense, 5'-AGA AGC ACT GCA GAG ACA TGG A-3', 5'-GGC GGG CTG CAT CCA-3', 5'-GCG CGG CGA TCA AGA A-3'; (2) antisense, 5'-CAC CTC TTG CCA CTC GTA CTT G-3', 5'-AGT GGT GTC TCG GTG ACA AAG TC-3', 5'-GAC ATC GCC CGA CGA CTT-3'; (3) β-actin sense, 5'-GCA TGG GTC AGA AGG ATT CCT-3'; and (4) antisense, 5'-TCG TCC CAG TTG GTG ACG AT-3'.

Second, the cells were placed into 1.5 ml Eppendorf tubes, adding TRIZol (Invitrogen Corporation) 1 ml and chloroform 0.2 ml, followed by shaking with force for 15 s, incubating (25 ^{o}C) for 3 min, centrifuging (4^{o}C, 12000 r/mins) for 15 min, and then taking on supernatant to the new 1.5 ml Eppendorf tubes, increasing isopropanol in the same volume of the supernatant. Subsequently, the samples were incubated for 10min at 25 ^{o}C and centrifuged (12000 r/min) for 10 min at 4 ^{o}C. Then 75% ethanol (including DEPC (diethypyrocarbonate) water) was performed to wash the precipitate (at least 1.0 ml 75% ethanol/ml TRIzol), and centrifuged (4 ^{o}C 7500 r/min) for 5 min. Finally, the disposable ethanol was precipitated with air-drying for 5-10 min (not completely dry), and DEPC treated water was added to dissolve RNA, followed by preserving at -80 ^{o}C.

Third, 4 μl RNA was performed to reverse-transcribe using ABI 9700 PCR instrument. The reaction condition was 1h at 37 ^{o}C, and then 3 min at 95 ^{o}C. Last, the p27, p21 gene transcription were amplified in 40 cycles, each consisting of 30 s at 93 ^{o}C for denaturation, 45 s at 55 ^{o}C for annealing, and 45 s at 72 ^{o}C for extension, followed by an extension for 5 min at

72 °C.

Co-immunoprecipitation (Co-IP) analysis

Total proteins were extracted from HeLa and HeLa p57 shRNA cells in an extraction buffer (50 mM Tris-HCl, pH 7.5-8.0, 100 mM NaCl, 1% NP-40, 0.5% sodium deoxycholate, 0.1%SDS, 1 mM EDTA, 1 mM sodium orthovanadate, 50 mM sodium fluoride, 1 mM PMSF, containing protease inhibitor cocktail (Roche)). Proteins extracts were inoculated with antibody for 4 h, and then protein A beads were added. After incubation, overnight at 4 °C, the beads were centrifuged and washed four times with a wash buffer (PBS, pH 7.4). The immunoprecipitated proteins were detected by SDS-PAGE gel separately with Cyclin E and Cyclin D1 antibody. Endogenous CDK2, CDK4 or CDK6 protein was detected with a rabbit polyclonal anti-CDK2, anti-CDK4 or anti-CDK6 antibody after immunoprecipitation with Cyclin E or Cyclin D1 antibody.

RNAi

Viral vectors are designed and constructed by Shanghai Jikai Gene Company. Then the RNAi lentiviral was added into the HeLa cells in logarithmic growth phase, making the slow virus to infect the HeLa cells. The relative nonspecific shRNA was set up as control group for each sample. After 8 hours' co-culture, the serum medium was added into the cultured cells, then after 3-4 days, infection efficiency was checked through GFP protein expression. 6-7 days later, interference efficiency was detected by RT-PCR and immunoblotting analysis.

Chips

After HeLa and HeLa p27 shRNA cells induced by the free and immobilized TNF-α plus IFN-γ for 24, 72, 144 hours, 0.25% trypsin (W/V) was performed to digest the HeLa and HeLa p27 shRNA cells. Then the HeLa and HeLa p27 shRNA cells were centrifuged by 4 °C, 1000 r/min for 5-10 min. The HeLa and HeLa p27 shRNA cells were collected and added 3 ml pre-cooling 4 °C PBS (-) to rinse the precipitation for two times, then centrifuged by 4 °C, 1000r/min for 5min. After detaching the supernatant, RNA Extraction Kit was added, stored in -80 °C for sending samples to Beijing BoAo biotechnology limited company for microarray

experiments.

Serological detection

We used the sterilized scissors to take blood samples from the tails of tumor-bearing nude mice treated by intravenous injection of three groups every other day. Before this procedure, a hair dryer blowing was used for tumor-bearing nude mice to get the blood circulation faster. For each animal, 1.5 ml blood was obtained and preserved in EP tube adding anticoagulants. When blood taking was completed, all the samples were sent to Guangdong laboratory animals monitoring institute (Guangzhou, China), to carry out the serum detection including the white blood cells (WBC), blood platelets (PLT), and red blood cells (RBC).

Prussian blue staining

Paraffin embedded tissue was placed in water. Hydrochloric acid and potassium ferrocyanide solution in 151 volume mixing ratios was freshly prepared and used to be working solution. Sections were immersed in working solution for standing 10–30 min. After the reaction, sections were immersed in distilled water for 3min and 3 times, and then rinsed thoroughly. Nuclear fast red solution was dropped in, covering the specimen for 5–10 min. After the reaction, sections were immersed in distilled water for 3 min and 3 times. And then sections were immersed in 95% alcohol and xylene to dehydrate for 2 min. The mounting medium was dropped onto the sections and covered with coverslip.

Additional Results

1. IFN-γ. Long-term cell cycle arrest and Bcl-2 family protein expression after p27 silencing.

Next, we investigated the p27 and p21 mRNA levels; the data are plotted in Figure S1A. A remarkable enhancement of the p27 mRNA level was observed in the C-group at 72 h and 144 h, with the maximal reached at 72 h. However, no such enhancement was observed in the F-group. A further determination of the levels and locations of p21 and p27 in the C- and F-groups was then necessary, in order to examine their roles in the G_1 arrest. In this case, the cells were stained with either an antibody that recognizes nuclear and cytoplasmic p21, or with a p27 antibody, followed by a secondary antibody with cyanine 3(Cy3). The expression of p21/p27 is depicted as red fluorescence. DAPI was used for nuclear staining (blue). As expected, in the C-group, p21 appears inside the nucleus (Figure S1B), while p27 mainly exists in the cytoplasm, indicating that the up-regulation of p21 may be one reason for the HeLa cell cycle G_1 arrest.

The expression of CDKI proteins in the HeLap27shRNA cells and the immunoblotted data are plotted in Figure S1D. Since the key proteins that modulate the apoptotic responses of p53, Bax, and Bcl-2, are sensitive to drug mediation, remarkable change was expected in the p53, Bax, and Bcl-2 levels in the C-group, after sufficient culture. The obtained data clearly indicate the remarkable down-regulation of p53 and Bax expression in this group. Nevertheless, an up-regulation of Bcl-2 expression was also detected. These results differ from those of the F-group. In parallel, the regulation behaviors of p53, Bax, and Bcl-2 expressions in the F- and C-groups with HeLa cells were similar, although p53 expression in the C-group became slowly up-regulated after being cultured for 72 h (Figure 2).

In order to avoid the unnecessary interruption from the shRNAi while p27 or p57 being silenced, a nonspecific shRNA was employed during our experiments. The results in Figure S1E indicate that the tendency of HeLa cells treated with this nonspecific shRNA is similar to the one of the original HeLa cells in Figure 2A, namely there are no influence occurring because of this shRNA.

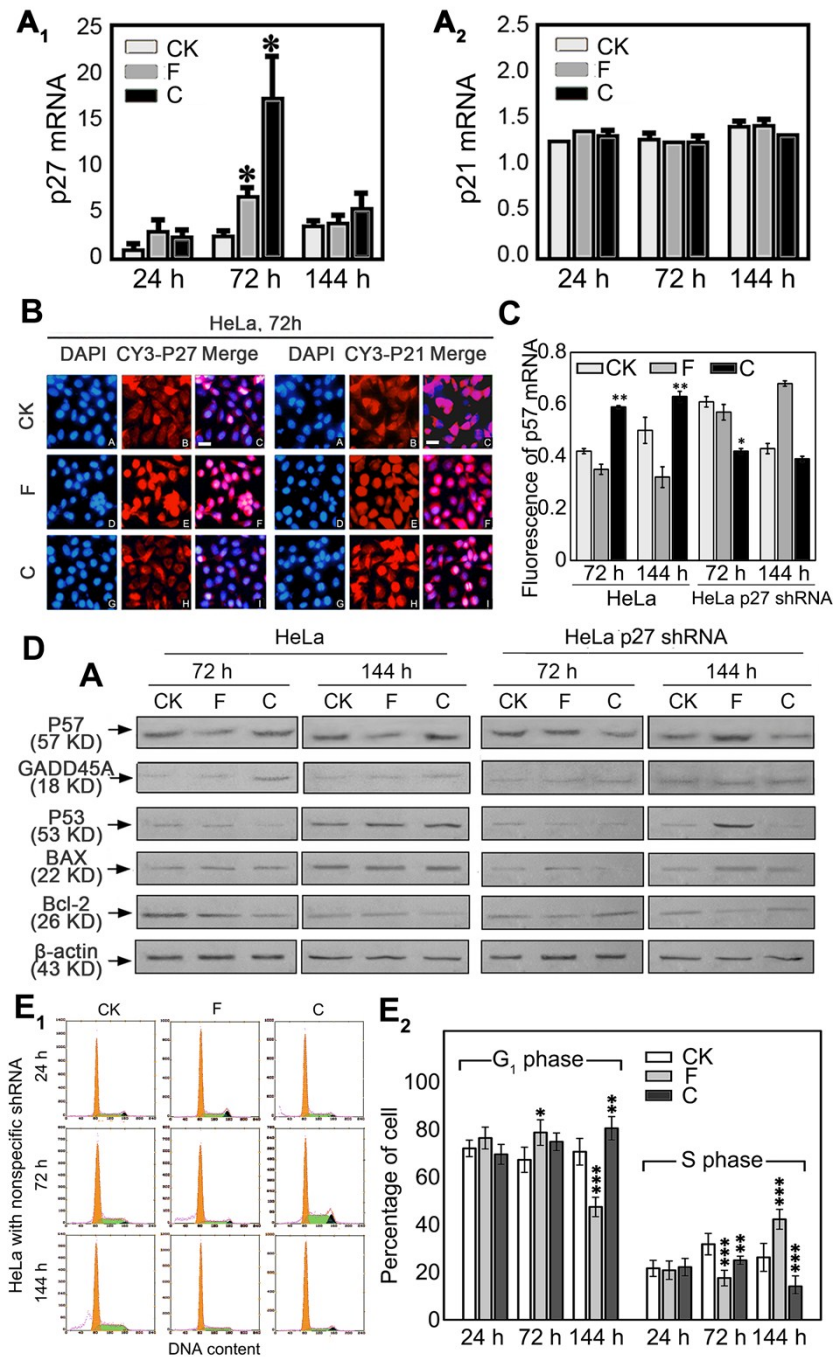

Figure S1. The expression of p27 and p21 was regulated, and cell cycle G_1 long arrest was induced by co-immobilized TNF-α plus IFN-γ. (A) Measured mRNA expression data of p27 (A_1) or p21 (A_2) real-time fluorescent quantitative PCR analysis for HeLa cells treated with free and co-immobilized TNF-α plus IFN-γ for 24 h, 72 h, and 144 h, respectively. (B) shows the protein subcellular redistribution data of p27 or p21 (white bars: 10 μm) by immunofluorescence for HeLa cells. (C) Measured mRNA expression data of p57 by real-time fluorescent quantitative PCR analysis for HeLa cells. (D) Measured protein expression data of p57, GADD45A, p53, Bax and Bcl-2, by western blotting for HeLa and HeLa p27 shRNA cells. (E_1) Measured cell cycle data of HeLa cells treated with a nonspecific shRNA by flow cytometry. (E_2) Evaluated cell percentages in the G_1 and S phase of cell cycle for the corresponding treatments.

2. p27 secondhand regulation role analysis and GADD45A is the other key factor.

Moreover, the gene chip data provided critical information on the top 15 coincident points, from which the direct reason for the long-term HeLa cell cycle arrest at G_1 may be clearly identified. Of particular interest among these coincident points is p57 (CDKNIC). The role of the p57 (CDKNIC) in the C- and F-groups was evaluated by analyzing the immunoblotting and RT-PCR data, as shown in Figure S1C. We examined the p57 mRNA levels in the C-group, cultured for 72 h and 144 h, as shown in Figure S1C. The p57 gene expression was up-regulated with increasing expression directly correlating to increased culture time. In the meantime, the p57 protein expression of the two C-groups with wild type and silent p27, cultured for 72 h and 144 h, are plotted in Figure S1D. In contrast to the two F-groups with wild type and silent p27, the cultured C-group with wild type p27 clearly displayed an up-regulation of p57 expression, which was down-regulated in the C-group with silent p27. This suggests that p57 is down-stream of p27 (Figure 3E). In addition, p57 expression was up-regulated in the F-group with silenced p27, indicating that p57 and p27 may play similar roles in the regulation of the cell cycle, but in different pathways.

The gene chip analysis also revealed another suspicious gene, GADD45A, which is down-stream of p27, as shown in Figure S1. GADD45A may play a similar regulatory role as p57. We investigated GADD45A protein expression in the two C-groups with wild type and silenced p27, cultured for 72 h and 144 h, as shown in Figure 2. A remarkable up-regulation of GADD45A gene expression was identified, differing from the observations of the F-group with wild type p27. In the C-group with silenced p27, however, GADD45A protein expression was down-regulated. Therefore, we suggest that both p57 and GADD45A are key factors for the observed long-term cell cycle arrest, down-stream from p27.

3. Microarray analysis of HeLa and HeLa p27 shRNA cells for cell cycle genes

The data presented above allow a clear indication that the HeLa cells in the C-group exhibit quite different behaviors from those in the other two groups. This stimulates us to go into the subsequent cell biology level. As seen, the p27 in the C-group mainly appears in the cytoplasm and the regulation of the p27 seems to be the important reason for the HeLa cell cycle G_1 long arrest. Unfortunately, this mechanism is indirect and an exploration of the direct

mechanism is challenging.

We then employ the gene chip technique to figure out the cell cycle progression regulation. We may compare the gene chip spectra from the two C-groups with the wild and silent p27 respectively. The data are summarized in Figure S2-S3, where the detailed analysis is presented in Figure S2A and B, and the clustering figures of the two chips are given in Figure S2C. These evaluated data include the top 25 up-regulated genes in the C-group with wild p27 and the top 25 down-regulated genes in the C-group with silent p27, as well as the top 15 coincident points which are up-regulated in the C-group with wild p27 and down-regulated in the C-group with silent p27.

A

Chip 1. Over-expression genes in HeLa treated with co-immobilized compared with free TNF-α/IFN-γ

	Gene Name	Fold change	Gene description
1	GADD45A	1.4562	Growth arrest and DNA-damage-inducible protein GADD45 alpha
2	RAD51	1.4019	DNA repair protein RAD51 homolog 1
3	CUL4B	1.3415	Cullin homolog 4B
4	CDC2	1.3311	Cell division control protein 2 homolog
5	CDK2	1.2537	Cell division protein kinase 2
6	CCNE1	1.2410	G1/S-specific cyclin E1
7	CDK4	1.2276	Cell division protein kinase 4
8	CUL2	1.2087	Cullin homolog 2
9	CDKNIC (p57)	1.2024	Cyclin-dependent kinase inhibitor 1C
10	SUMO1	1.1868	Ubiquitin-like protein SMT3C precursor
11	CUL1	1.1839	Cullin homolog 1
12	RB1	1.1825	Retinoblastoma-associated protein
13	CDC37	1.1767	Hsp90 co-chaperone Cdc37
14	CCNB1	1.1734	G2/mitotic-specific cyclin B1
15	CUL4A	1.1687	Cullin homolog 4A
16	STAT6	1.1319	Signal transducer and activator of transcription 6
17	SKP2	1.1227	S-phase kinase-associated protein 2
18	CDC20	1.0865	Cell division cycle protein 20 homolog
19	E2F2	1.0722	Transcription factor E2F2
20	CDC6	1.0700	Cell division control protein 6 homolog
21	CDKN1A	1.0597	Cyclin-dependent kinase inhibitor 1 (p21)
22	CDKN1B	1.0592	Cyclin-dependent kinase inhibitor 1B
23	RBL2	1.0544	Retinoblastoma-like protein 2
24	CDK6	1.0537	Cell division protein kinase 6
25	STAT5B	1.0261	Signal transducer and activator of transcription 5B

B

Chip 2. Under-expression genes in HeLa p27 shRNA compared with HeLa treated with co-immobilized TNF-α/IFN-γ

	Gene Name	Fold change	Gene description
1	GADD45A	0.4733	Growth arrest and DNA-damage-inducible protein GADD45 alpha
2	CDKN1A	0.5524	Cyclin-dependent kinase inhibitor 1 (p21)
3	ATM	0.6342	Serine-protein kinase ATM
4	CDK8	0.6332	Cell division protein kinase 8
5	CCNG2	0.7020	Cyclin G2
6	CDKN1B	0.7031	Cyclin-dependent kinase inhibitor 1B (p27Kip1)
7	SKP2	0.7524	S-phase kinase-associated protein 2
8	CHEK2	0.7685	Serine/threonine-protein kinase Chk2
9	CUL2	0.7774	Cullin homolog 2
10	E2F2	0.7808	Transcription factor E2F2
11	RBL2	0.8421	Retinoblastoma-like protein 2
12	CDKN2B	0.8503	Cyclin-dependent kinase 4 inhibitor B
13	CDC34	0.8652	Ubiquitou-conjugating enzyme E2-32 kDa complementing
14	CUL4B	0.8723	Cullin homolog 4B
15	KNTC1	0.8842	Kinetochore-associated protein 1
16	CCNC	0.8842	Cyclin C
17	CDKNIC (p57)	0.8850	Cyclin-dependent kinase inhibitor 1C
18	RAD9A	0.9290	RAD9 homolog (S. pombe)
19	CDC7	0.9300	Cell division cycle 7-related protein kinase
20	CCND1	0.9301	G1/S-specific cyclin D1
21	ATR	0.9486	ataxia telangiectasia and Rad3 related protein
22	RB1	0.9718	Retinoblastoma-associated protein
23	CDC25C	0.9810	M-phase inducer phosphatase 3
24	BRCA1	0.9852	Breast cancer type 1 susceptibility protein
25	CDK4	0.9997	Cell division protein kinase 4

C

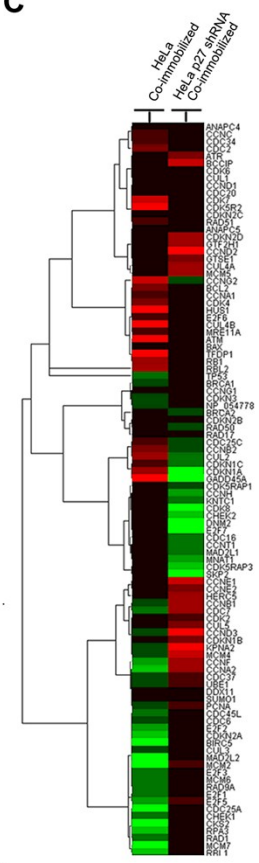

Figure S2. Microarray analysis of HeLa and HeLa p27 shRNA cells for cell cycle genes. (A) the over-expressed 25 genes in HeLa treated with co-immobilized TNF-α plus IFN-γ compared with free TNF-α plus IFN-γ; (B) the under-expressed 25 genes in HeLa treated with co-immobilized TNF-α plus IFN-γ compared with free TNF-α plus IFN-γ; (C) the gene dendrograms.

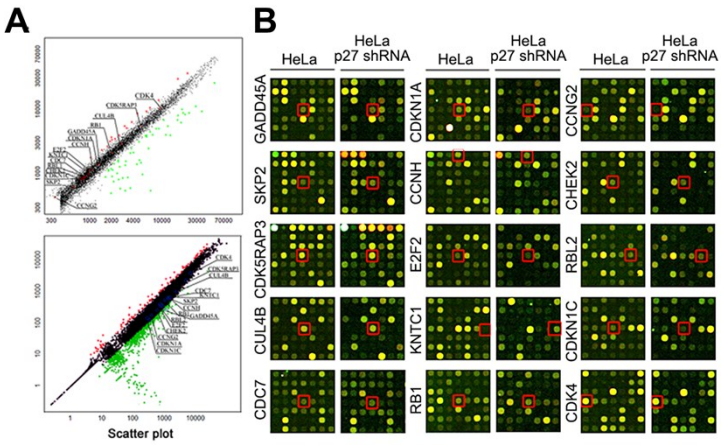

C

Under-expression cell cycle genes in HeLa cell without p27

	Gene name	chip 2	chip 1	Gene function
1	**GADD45A**	0.4733	1.4562	cell cycle arrest
2	CDKN1A	0.5524	1.0597	apoptosis
3	CCNG2	0.7020	1.1750	nuclear division
4	SKP2	0.7524	1.1227	mitotic cell cycle
5	CCNH	0.7666	1.0030	transcription, DNA-dependent
6	CHEK2	0.7685	1.0241	response to stress
7	CDK5RAP3	0.7709	1.0652	regulation of development
8	E2F2	0.7808	1.0722	transcription initiation
9	RBL2	0.8421	1.0544	regulation of cell cycle
10	CUL4B	0.8723	1.3415	cell growth and/or maintenance
11	KNTC1	0.8842	1.0605	regulation of exit from mitosis
12	**CDKNIC (p57)**	0.8850	1.2024	negative regulation of cell cycle
13	CDC7	0.9300	1.0470	regulation of cell process
14	RB1	0.9718	1.1825	negative regulation of cell cycle
15	CDK4	0.9997	1.2276	macromolecule matabolism

Figure S3. Microarray analysis of HeLa and HeLa p27 shRNA cells for cell cycle genes. (A) the scatter diagrams (HeLa treated with co-immobilized TNF-α plus IFN-γ compared with free TNF-α plus IFN-γ (top), HeLa treated with co-immobilized TNF-α plus IFN-γ compared with HeLa p27 shRNA treated with co-immobilized TNF-α plus IFN-γ (bottom); (B) the chip images of 15 cell cycle relative genes which were changed significantly in two chips; (C) the gene function descriptions of 15 cell cycle relative genes which were changed significantly in two chips.

4. Regulation of p27 and p57 expression in the other cervix cancer cells

Figure S4-S5 shows the inhibition effect of co-immobilized TNF-α plus IFN-γ to SiHa and CaSki cells. As shown in Figure S4A, when induced for 72 h, the cell death of co-immobilized TNF-α plus IFN-γ was higher than other two groups. The result is more obvious than 72 h when induced for 144 h. It is concluded that the co-immobilized TNF-α plus IFN-γ group can also induce SiHa or CaSki cells death obviously, and as the extension of time, the cell death was more obvious. Moreover, by 72 h and 144 h stimulation, we collected these cells for flow cytometric analysis.

Figure S4B$_1$ and B$_2$ show that, when induced for 72 h, cell cycle arrest was not distinct compared to the free group. But when induced for 144 h, G_1 phase number in co-immobilized was evidently compared to the other two groups (***, P<0.001). It suggests that co-immobilized TNF-α plus IFN-γ can also strongly induce G_1 long arrest in the other cervix cancer cells.

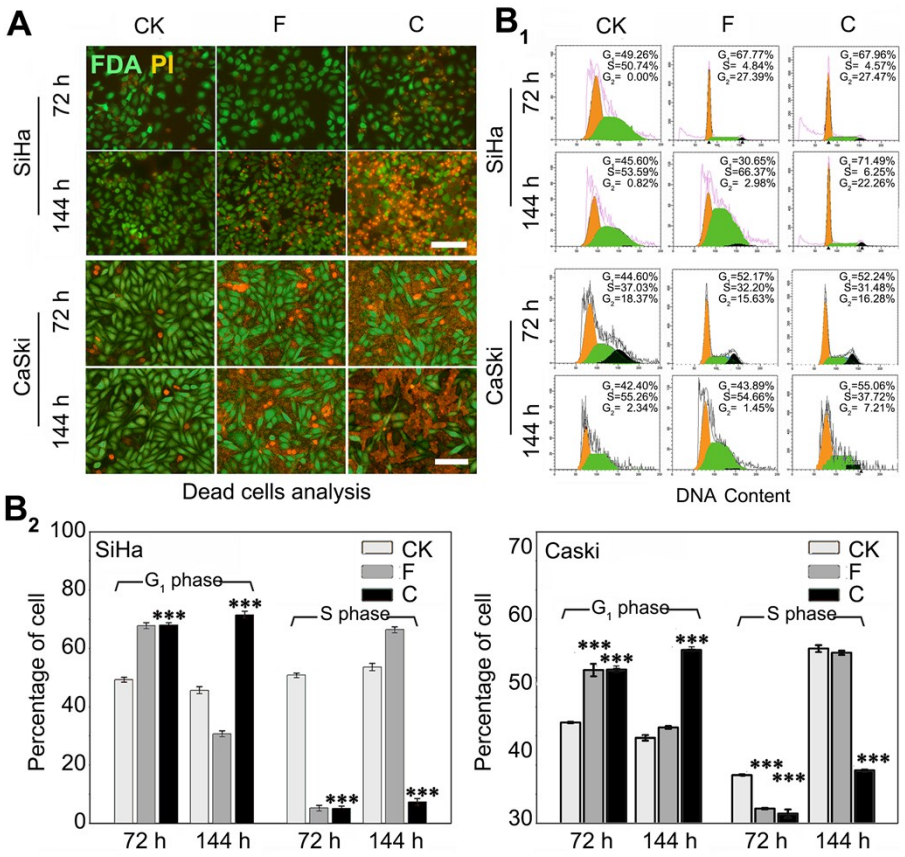

Figure S4. p27 and p57 regulation role analysis for SiHa or CaSki cells were treated with co-immobilized TNF-α plus IFN-γ for 72 h and 144 h. (A) Measured cell death for cells. The length bar=40 μm. (B$_1$) Measured cell cycle data by flow cytometry. (B$_2$) Evaluated cell percentages in the G_1 and S phase of cell cycle for the corresponding treatments. The relative levels are plotted with the significance p<0.05 labeled by symbol * and p<0.001 labeled by symbol **, in comparison with the control group. The bars stand for the standard deviations (n=3).

Then after 72 h and 144 h stimulation, the RT-PCR results show that the expressions of p27 and p57 in mRNA level in co-immobilized were both highest in three groups as shown in Figure S5A. These results were consistent with RT-PCR results of HeLa cells. However, the results of western blotting show that the expression of P27 in protein level in co-immobilized

were the lowest. For P57, when induced for 72 h, the expression of P57 in protein level in co-immobilized was the lowest, but when induced for 144 h, the protein level was the highest, as shown in Figure S5B.

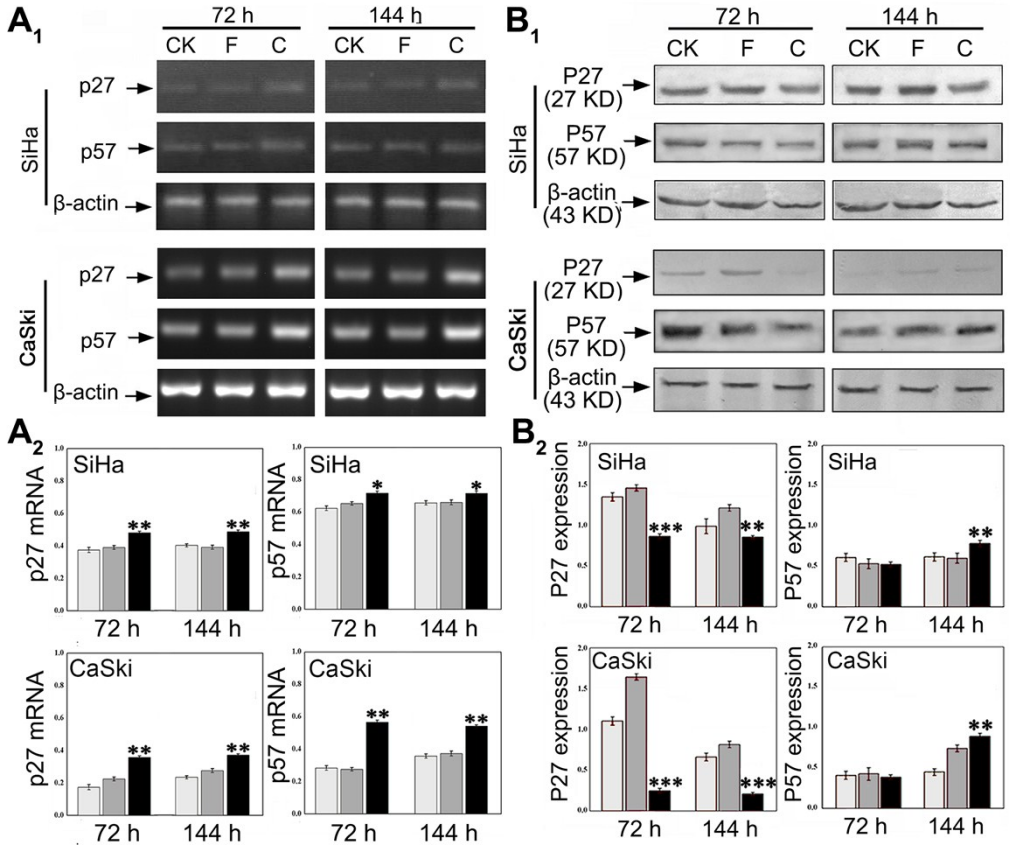

Figure S5. p27 and p57 regulation role analysis for SiHa or CaSki cells were treated with co-immobilized TNF-α plus IFN-γ for 72 h and 144 h. (A_1-A_2) Measured mRNA expression data of p27 and p57 by real-time fluorescent quantitative PCR analysis for SiHa or CaSki cells. Blots were reprobed for β-actin and used as control for equal loading of proteins. The mRNA expression was determined using BandScan software. (B_1-B_2) Measured protein expression data of p27 and p57 by western blotting for SiHa or CaSki cells. Blots were reprobed for β-actin and used as control for equal loading of proteins. The protein expression was determined using BandScan software. The relative levels are plotted with the significance $p<0.05$ labeled by symbol * and $p<0.001$ labeled by symbol **, in comparison with the control group. The bars stand for the standard deviations (n=3).

5. Effect of nano-drug on tumor progression and toxicities data in nude mice models.

We then assessed the toxicity of the nano-drug in nude mice by counting white blood cells (WBC), blood platelets (PLT), and red blood cells (RBC). The results showed no significant difference when compared with the normal index, implying that there is no toxic effect *in vivo* (Figure S6A). At the same time, almost no multi-target MNPs were found in

other tissues, which is evidenced by the morphology of the hearts, livers, spleens, lungs, and kidneys shown in Figure S6B. Thus, all of these data indicate that the nano-drug can effectively inhibit tumor growth and reduce the mortality of tumor-burdened nude mice, without toxic effects.

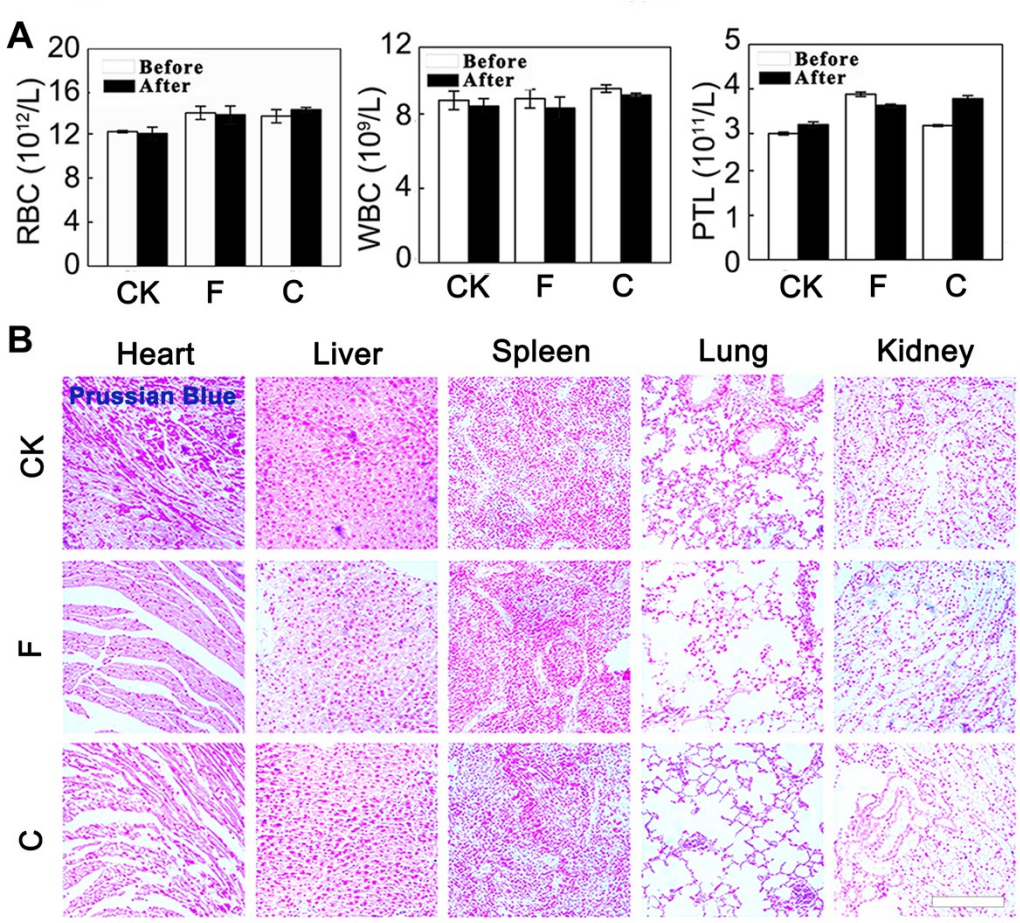

Figure S6. Effect of nano-drug on tumor progression and toxicities data in nude mice models. (A) Serological and toxicology test of nude mice, including the density of red blood cell (RBC, left), the density of white blood cell (WBC, middle), and the density of platelet (PLT, right), upon the treatment. Significant increase or decrease at labels (*) ($P < 0.05$), labels (**) ($0.001 < p < 0.01$) and labels (***) $p < 0.001$, are identified in comparison with the CK-group. The bars stand for the standard deviations (n=6). (B) Prussian blue staining of five normal tissues upon the treatment. The length bar=100 μm.